Heliyon 10 (2024) e36991

Contents lists available at ScienceDirect

Heliyon

journal homepage: www.cell.com/heliyon

Research article

MDD brain network analysis based on EEG functional connectivity and graph theory

Wan Chen, Yanping Cai [*], Aihua Li, Ke Jiang, Yanzhao Su

Rocket Force University of Engineering, Xi'an, 710025, China

ARTICLE INFO

Keywords:
EEG
Major depression disorder
Functional connectivity
Graph theory

ABSTRACT

Background: Existing studies have shown that the brain network of major depression disorder (MDD) has abnormal topologies. However, constructing reliable MDD brain networks is still an open problem.
New method: This paper proposed a reliable MDD brain network construction method. First, seven connectivity methods are used to calculate the correlation between channels and obtain the functional connectivity matrix. Then, the matrix is binarized using four binarization methods to obtain the EEG brain network. Besides, we proposed an improved binarization method based on the criterion of maximizing differences between groups: the adaptive threshold (AT) method. The AT can automatically set the optimal binarization threshold and overcome the artificial influence of traditional methods. After that, several network metrics are extracted from the brain network to analyze inter-group differences. Finally, we used statistical analysis and Fscore values to compare the performance of different methods and establish the most reliable method for brain network construction.
Results: In theta, alpha, and total frequency bands, the clustering coefficient, global efficiency, local efficiency, and degree of the MDD brain network decrease, and the path length of the MDD brain network increases.
Comparison with existing methods: The results show that AT outperforms the existing binarization methods. Compared with other methods, the brain network construction method based on phase-locked value (PLV) and AT has better reliability.
Conclusions: MDD has brain dysfunction, particularly in the frontal and temporal lobes.

1. Introduction

Major depression disorder (MDD) is a common mental illness that can lead to reduced cognitive ability [1–3]. In severe cases, people with MDD may even become suicidal. According to the World Health Organization, more than 300 million people in the world are suffering from depression [4]. As the number of patients with MDD continues to increase, understanding the underlying neurophysiological mechanisms is critical to the diagnosis and treatment of MDD.

EEG can reflect the activity of the human brain and is an objective and reliable physiological indicator. In addition, EEG has been widely used to assess brain activity in MDD due to its advantages such as high time resolution, low cost, simple operation, and non-trauma [5–7]. Many EEG-based physiological indicators have been used to evaluate MDD brain activity, such as time-domain [8],

* Corresponding author.
E-mail address: caiyanping502@163.com (Y. Cai).

https://doi.org/10.1016/j.heliyon.2024.e36991
Received 9 January 2024; Received in revised form 26 August 2024; Accepted 26 August 2024
Available online 27 August 2024

frequency-domain [9], non-linear EEG features [10]. The results show that MDD has a higher energy in the alpha band, which can be considered as a potential biomarker of MDD [11]. However, the above methods tend to treat the electrodes as isolated points, ignore the correlation between the electrodes, and fail to reveal the brain topological changes in MDD [12].

Graph theory analysis based on functional connectivity provides important information for the topological properties of brain networks [13]. More and more studies have shown that MDD presents abnormal brain network structure [14–16]. Li et al. [13] used coherence (Coh) to construct the functional connectivity matrix, and adopted minimum spanning tree (MST) to achieve the binarization of the functional connectivity matrix. The experimental results show that the Coh of MDD is significantly higher than that of normal control (NC). Liu et al. [14] used Coh to construct the functional connectivity matrix, and then set a threshold to convert the weighted matrix into a binary matrix. The statistical analysis results show that the clustering coefficient (CC) and path length (PL) of MDD are lower than those of NC. Shao et al. [17] built the functional connectivity matrix using correlation, Coh and phase lag index (PLI), and converted the weighted matrix into a binary matrix using density method, from which CC, PL and small-world index were extracted. The statistical results show that the CC of MDD is significantly lower than that of NC. Zhang et al. [18] used the PLI to construct the functional connectivity matrix, and realized the binarization of the weighted matrix using a threshold. The results show that the path length of MDD increases and the clustering coefficient decreases. However, few studies have compared the performance of different methods in analyzing MDD brain networks [19–21].

Various connectivity methods have been applied to construct brain networks [17–19]. Pearson correlation coefficient (PCC) [22] and Coh [13,14] measure the correlation of two signals in the time and frequency domains. However, both PCC and Coh can only detect linear correlations between signals. Mutual information (MI) [23] measures the correlation of two signals from the information theory, and can simultaneously detect the linear and nonlinear correlation of two signals. However, MI is greatly affected by signal noise. Phase-locked value (PLV) [24] and PLI [25] are phase-based connectivity methods. Existing studies have shown that PLV is sensitive to volume conduction. The PLI has a certain robustness to volume conduction, but is sensitive to noise in the signal [26]. Besides, there are some connectivity methods that are insensitive to volume conduction and noise, such as imaginary part coherence (ICoh) [27], weighted phase lag index (WPLI) [28].

The functional connectivity matrix computed using the connectivity method is a weighted matrix. The weighted matrix usually contains false connections, which is not conducive to brain network analysis [24]. The weighted matrix can be transformed into a binary matrix using a binarization method, which can eliminate spurious connections and minimize noise. Therefore, analyzing brain network topology based on binary networks has received more attention [29]. The most common binarization methods include the threshold method and density method [12,17]. The threshold method determines the existence of connected edges by a threshold [18,30]. However, the selection of threshold value has a large subjective factor [12]. Moreover, some studies have pointed out that threshold method will lead to differences in the number of connections in brain networks, which may affect the analysis of brain networks [24]. The density method can ensure that the number of connected edges in all brain networks is consistent using an appropriate network density to extract the connected edges [19,31]. However, the selection of network density is also highly subjective [22]. The minimum spanning tree (MST) is an unbiased binarization method, which can avoid the subjectivity of threshold method and density method, and has been successfully applied to brain network analysis [13,32]. However, MST produces a highly sparse brain network that may be missing some important connections [19]. The minimum connection component (MCC) is also an unbiased binarization method, which can avoid the sparsity problem of the MST to a certain extent [29]. However, the performance of MCC in MDD brain network analysis is still to be explored. Therefore, how to design a reliable MDD brain network analysis method is still an urgent problem to be solved.

This paper aims to build a reliable MDD brain network construction method to provide a basis for MDD brain activity analysis and MDD diagnosis. Different connectivity calculation methods and binarization methods will affect the reliability of brain network construction. However, most existing studies have selected the brain network construction method based on personal experience, which lacks the necessary theoretical and experimental basis. Therefore, this paper compared the performance of existing connectivity and binarization methods to provide a reference for MDD brain network construction and MDD diagnosis. Besides, the traditional threshold method has a lot of human factors and cannot guarantee the optimal threshold value. This paper proposed an adaptive threshold method based on the principle of maximizing the difference between groups. The adaptive threshold method can automatically optimize the binarization threshold and avoid the influence of human factors. The specific contributions of this paper are as follows.

(1) Adaptive threshold (AT) and adaptive density (AD) algorithms are proposed, which can realize the adaptive setting of threshold and density and maximize the difference of brain network between MDD and NC. The results show that AT outperforms the existing binarization methods.
(2) Comparing the performance of different connectivity methods (Coh, ICoh, MI, PCC, PLI, PLV, WPLI) and binarization methods (AT, AD, MST, MCC) in MDD brain network analysis, the results show that PLV + AT is a reliable method for MDD brain network analysis.
(3) The MDD brain network changes are analyzed from multiple aspects, and the results show that the connectivity of the MDD brain network decreased significantly in theta, alpha and total bands, especially in the frontal and temporal lobes.

2. Method

Fig. 1 shows the research idea of this paper. First, the EEG is pre-processed, including EEG artifact removal, segmentation, and frequency band extraction. Graph theory is then used to analyze the brain networks of MDD, including constructing the functional connectivity matrix, computing the binary matrix, and extracting the brain network metrics. Meanwhile, we propose AT and AD algorithms based on quantum particle swarm optimization (QPSO) to avoid the effect of artificial thresholds. Finally, brain network metrics are statistically analyzed to explore changes in MDD brain networks.

2.1. Construction of functional connectivity matrix

A network consists of nodes and edges connecting nodes to each other. In this study, EEG electrodes are defined as nodes and the connectivity strength between different EEG electrodes is defined as the connecting edge. Therefore, for an EEG with N channels, a functional connectivity matrix with dimension N × N can be obtained using the connectivity method. To explore a reliable method for MDD brain network analysis, seven connectivity methods are used in the study, including Coh, ICoh, MI, PCC, PLI, PLV, WPLI.

(1) Coherence and imaginary part coherence

Coh can measure the linear correlation of two signals in the frequency domain, which has been widely used to calculate functional connectivity [13,14]. For signals x and y, Coh and ICoh are calculated as shown in Equations (1) and (2).

$$Coh_{xy}(f) = \frac{\left|p_{xy}(f)\right|}{\sqrt{p_{xx}(f)p_{yy}(f)}} \tag{1}$$

$$ICoh_{xy}(f) = \frac{im\left(p_{xy}(f)\right)}{\sqrt{p_{xx}(f)p_{yy}(f)}} \tag{2}$$

Where f represents the frequency, $p_{xy}(f)$ represents the mutual power spectral density of signal x and y, $p_{xx}(f)$ represents the power spectral density of x, $p_{yy}(f)$ represents the power spectral density of signal y, and $im(\cdot)$ represents the imaginary part.

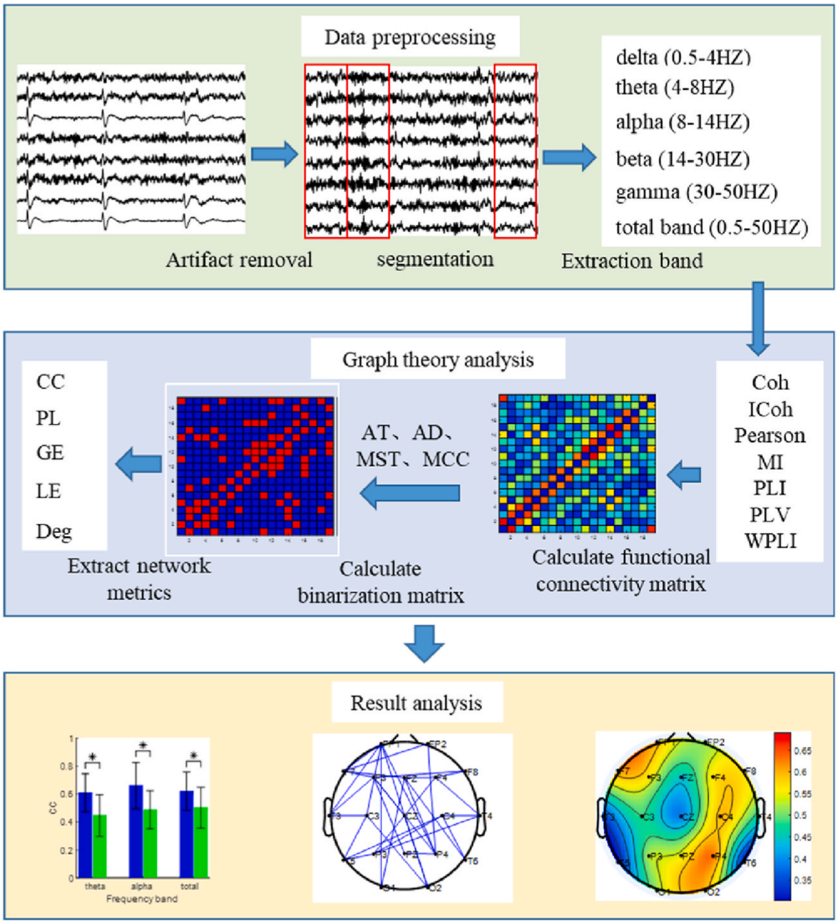

Fig. 1. Flow chart of MDD brain network analysis method.

(2) Mutual information

MI measures the dependence of two signals from information theory, and can simultaneously detect the linear and nonlinear correlation of two signals [23]. The larger the value of MI, the greater the correlation between the two signals. For signals x and y, MI is calculated as shown in Equation (3).

$$MI_{xy} = \sum_{x_i \in x, y_j \in y} p\left(x_i, y_j\right) \log \frac{p\left(x_i, y_j\right)}{p(x_i) p\left(y_j\right)} \tag{3}$$

Where, $p\left(x_i, y_j\right)$ represents the joint probability distribution function of signals x and y. $p(x_i)$ and $p\left(y_j\right)$ represent the edge probability distribution function of signals x and y, respectively.

(3) Pearson correlation coefficient

PCC can measure the linear correlation of two signals in the time domain [22]. The greater the absolute value of the PCC, the stronger the correlation between the two signals. For signals x and y, PCC is calculated as shown in Equation (4).

$$PCC_{xy} = \frac{\sum_{i=1}^{n} (x_i - \overline{x})(y_i - \overline{y})}{\sqrt{\sum_{i=1}^{n} (x_i - \overline{x})^2} \sqrt{\sum_{i=1}^{n} (y_i - \overline{y})^2}} \tag{4}$$

(4) Phase lag index

PLI is a correlation measurement method based on phase, which can measure the asymmetry of phase distribution between two signals [17]. For signals x and y, PLI is calculated as shown in Equation (5).

$$PLI_{xy} = \left| \frac{1}{T} \sum_{t=1}^{T} sign\left(\varphi_{xy}(t)\right) \right| \tag{5}$$

Where $\varphi_{xy}(t)$ represents the phase difference between the signal x and y at time t, and $sign(\cdot)$ represents the symbolic function.

(5) Phase lock value

The PLV assumes that the amplitude and phase of the signal are statistically independent of each other, and only phase synchronization is used to estimate the functional interaction between the two electrode channels/brain region signals [11]. For signals x and y, PLV is calculated as shown in Equation (6).

$$PLV_{xy} = \left| \frac{1}{T} \sum_{t=1}^{T} e^{j\varphi_{xy}(t)} \right| \tag{6}$$

(6) Weighted phase lag index

WPLI can avoid the defect that PLI is easily disturbed by noise, and is often used to construct functional connectivity matrix [28]. For signals x and y, WPLI is calculated as shown in Equation (7).

$$WPLI_{xy} = \frac{\left| \frac{1}{N} \sum_{n=1}^{N} \left| im\left(S_{xy}^{n}\right) \right| sign\left(im\left(S_{xy}^{n}\right)\right) \right|}{\frac{1}{N} \sum_{n=1}^{N} \left| im\left(S_{xy}^{n}\right) \right|} \tag{7}$$

Where, S_{xy} represents the cross-power spectrum of signal x and y, $|\cdot|$ represents the absolute value, and N represents the data point.

2.2. Binarization of functional connectivity matrix

The correlation between different channels can be calculated and the functional connectivity matrix can be constructed using the connectivity method. The functional connectivity matrix is a weighted matrix and may contain spurious connections [24]. Therefore, binarization methods are often used to transform the weighted matrix into a binary matrix for analyzing brain networks. In this paper, four binarization methods are used, including MST, MCC, AT and AD.

(1) Minimum spanning tree

The MST of a graph is to choose N-1 connected edges from a network of N nodes to connect N nodes, and to minimize the sum of the weights of the N-1 edges. For EEG brain networks, important connected edges need to be extracted. Therefore, Kruskal algorithm is used to build the MST with the maximum sum of weights [13]. For a weighted network of N nodes, all connected edges are first ordered in descending order according to their weights. The connected edges are then added from top to bottom according to the weights. If the added connected edge causes the network to form a loop, this edge is skipped. This process is repeated until N-1 connected edges are chosen such that all N nodes are connected to a yacyclic subgraph. The weight of the selected N-1 connected edges is set to 1 and the weight of the remaining connected edges is set to 0 to achieve binarization of the weighted network.

(2) Minimum connection component

For a network of N nodes, MST will produce a sparse network with N-1 connecting edges, which may lead to the missing of some key connecting edges [19]. Therefore, Vijayalakshmi et al. [33] proposed a binarization method based on the MCC. MCC is a spanning tree with at least N-1 connected edges, which can overcome the sparsity problem of MST to some extent. For a weighted network of N nodes, the connected edges are first sorted in descending order according to their weights. Then, the connected edges are selected from top to bottom until a connected graph is obtained. The weights of the selected connected edges are set to 1 and the remaining weights are set to 0 to achieve binarization of the weighted network.

(3) Adaptive threshold and adaptive density

The threshold method can achieve the binarization of the weighting matrix setting an appropriate threshold [18]. The density method can achieve the binarization of the weighting matrix setting a suitable network density [19]. Both the threshold method and the density method require manual setting of parameters, which is subjective and may affect the construction of brain networks. Therefore, this paper proposes AT and AD algorithms based on QPSO, avoiding the manual setting of threshold and network density.

The greater the difference between MDD and NC, the more beneficial to brain network analysis. Therefore, the AT and AD algorithms aim to maximize the distance between the functional connectivity matrix of MDD and NC. In order to find the maximum distance between the functional connectivity matrix of MDD and NC, swarm intelligence optimization algorithms is used for optimization. Common swarm intelligence optimization algorithms include genetic algorithm (GA), particle swarm optimization (PSO), and QPSO [34,35]. QPSO has the advantages of few input parameters and not easily falling into local optimal, and has been widely used in many fields [36,37]. Therefore, in this paper, QPSO is chosen to find the optimal threshold and network density.

For samples $\{A_i, i = 1, 2, \ldots, k_a\}$ in MDD and samples $\{B_i, i = 1, 2, \ldots, k_b\}$ in NC, where A_i represents the functional connectivity matrix of i-th MDD and B_i represents the functional connectivity matrix of i-th NC. The AT is calculated as follows.

Step1 Initialize the particle swarm X using Equation (8).

$$X = x_{\min} + (x_{\max} - x_{\min}) \times rand(1, N) \tag{8}$$

Where $x_{\max}$ and $x_{\min}$ represent the upper and lower limits of the threshold, N represents the particle swarm size, and $rand(\cdot)$ represents the random number.

Step2 Transform the functional connectivity matrices A and B into binary matrices. Taking the j-th particle X_j as the threshold value, the functional connectivity matrix A of MDD is transformed into the binary matrix G_A, and the functional connectivity matrix B of NC is transformed into the binary matrix G_B.

Step3 Calculate the mean of $\{G_{A_i}, i = 1, 2, \ldots, k_a\}$ and $\{G_{B_i}, i = 1, 2, \ldots, k_b\}$ using Equations (9) and (10).

$$\overline{G}_A = \frac{1}{k_a} \sum_{i=1}^{k_a} G_{A_i} \tag{9}$$

$$\overline{G}_B = \frac{1}{k_b} \sum_{i=1}^{k_b} G_{B_i} \tag{10}$$

Step4 Calculate the distance between $\overline{G}_A$ and $\overline{G}_B$ using Equation (11) as the fitness value of X_j.

$$f_j = \sum_{m=1}^{l-1} \sum_{n=m+1}^{l} \left| \overline{G}_A^{mn} - \overline{G}_B^{mn} \right| \tag{11}$$

Step5 Repeat Step2-Step4 to obtain the individual historical optimum *Pbest* and the global optimum *Gbest* for the first generation of particles. The general equations are shown in (12)-(13):

$$Pbest = X \tag{12}$$

$$Gbest = X_{\max(f)} \tag{13}$$

Where $X_{\max(f)}$ represents the particle with the largest fitness value.

Step6 Update the particles using Equations (14)–(17).

$$P_i = \varphi \cdot Pbest_i + (1-\varphi) \cdot Gbest \tag{14}$$

$$m_{best} = \frac{1}{N}\sum_{i=1}^{N} P_i \tag{15}$$

$$\alpha = 0.5 + 0.5 \cdot (T_{\max} - T) / T_{\max} \tag{16}$$

$$x_i(t+1) = \begin{cases} P_i - \alpha \cdot |m_{best} - x_i(t)| \cdot \ln(1/u_i) & r \geq 0.5 \\ P_i + \alpha \cdot |m_{best} - x_i(t)| \cdot \ln(1/u_i) & r < 0.5 \end{cases} \tag{17}$$

Where $x(t)$ represents the t-th generation particle. φ, u and r represent random numbers in (0,1). α represents the contraction expansion coefficient. T represents the current iteration. $T_{\max}$ represents the maximum iteration.

Step7 Calculate the fitness value of the new particle set according to Step2-Step4.
Step8 Update the individual historical optimum and the global optimum using Equations (18) and (19).

$$Pbest_i = \begin{cases} X_i & f_{X_i} > f_{Pbest_i} \\ Pbest_i & else \end{cases} \tag{18}$$

$$Gbest = \begin{cases} X_k & f_{X_k} > f_{Gbest} \\ Gbest & else \end{cases} \tag{19}$$

Where X_k represents the particle with the largest fitness value in the current particle set.

Step9 Repeat Step6-Step8 until the termination condition is satisfied and the global optimum *Gbest* is output. *Gbest* is the adaptive threshold.

The calculation procedure of AD differs from that of AT in two ways: First, the particles in AD represent the network density. Second, AD uses the density method in Step2 to transform the functional connectivity matrix into a binary matrix.

2.3. Extract network metrics

Graph theory has been widely used to analysis the brain network topology in MDD [12]. In this paper, path length (PL), clustering coefficient (CC) [30], global efficiency (GE) [20], local efficiency (LE) [21] and degree (Deg) [14] are extracted from the brain network to analyze the topology of the brain network in MDD. The general equations are shown in (20)-(24). Brain network metrics are calculated using the Brain Connectivity Toolbox (BCT, http://www.brain-connectivity-toolbox.net/).

(1) Path length

The PL reflects the overall efficiency of information integration between different brain regions. The smaller the PL, the higher the information transmission efficiency of the network.

$$PL = \frac{1}{N}\sum_{i\in N}\frac{\sum_{j\in N, j\neq i} d_{ij}}{N-1} \tag{20}$$

Where d_{ij} represents the shortest path length between node i and node j.

(2) Clustering coefficient

CC is an important parameter to measure the degree of clustering and connectivity tightness in brain networks. The larger the CC, the more efficient the local information processing of the brain network.

$$CC = \frac{1}{N}\sum_{i=1}^{N}\frac{2E_i}{k_i(k_i-1)_i} \tag{21}$$

Where k_i represents the number of nodes connected to node i. E_i represents the actual number of edges between k_i nodes.

(3) Global efficiency

GE is a comprehensive measure of the speed of information transmission in brain networks. In contrast to PL, GE allows the network to have isolated points, which allows a more comprehensive description of the network features.

$$GE = \frac{1}{N}\sum_{i\in N}\frac{\sum_{j\in N, j\neq i}\frac{1}{d_{ij}}}{N-1} \tag{22}$$

(4) Local efficiency

Similar to CC, LE is also used to measure local features of the network. A higher LE indicates that the network is insensitive to small-scale faults.

$$LE = \frac{1}{N}\sum_{i\in N}\frac{\sum_{j,s\in G_i}\frac{1}{d_{js}}}{N_{G_i}\left(N_{G_i}-1\right)} \tag{23}$$

Where G_i represents the sub-graph composed of adjacent nodes of node i. N_{G_i} represents the number of nodes in the sub-network G_i.

(5) degrees

Degree is one of the simplest, most intuitive, and most important properties of nodes in complex network models. The larger the degree of a node, the more important that node is. The mean degree of the network can be obtained by averaging the degrees of all nodes.

$$D = \frac{1}{N}\sum_{i=1}^{N}\sum_{j=1}^{N}h_{ij} \tag{24}$$

Where h_{ij} represents the element of the binary matrix. $h_{ij} = 1$ indicates that there is a connection between node i and node j.

2.4. Result analysis

Statistical tests are used to explore whether there were differences between MDD and NC network metrics, including independent sample *t*-test and Wilcoxon rank sum test [14,38]. When the statistical test results of the two methods are both $P < 0.05$, it indicates that the results are statistically different. In addition, Fscore values are also used to evaluate the effectiveness of network metrics. Fscore is a common feature selection method and is also used for EEG feature selection [39]. The Fscore feature selection method achieves feature ranking by calculating the Fscore value of each feature. The larger the Fscore value, the better the performance of the feature. The Fscore value is calculated as shown in Equation (25). Where s and q represent two types of samples, u represents the mean value, i represents the number of features, x represents the feature, and k represents the number of samples.

$$F_i = \frac{\left(u_i^s - u_i\right)^2 + \left(u_i^q - u_i\right)^2}{\frac{1}{n_s-1}\sum_{k=1}^{n_s}\left(x_{k,i}^s - u_i^s\right)^2 + \frac{1}{n_q-1}\sum_{k=1}^{n_q}\left(x_{k,i}^q - u_i^q\right)^2} \tag{25}$$

3. Data acquisition and data preprocessing

3.1. Data acquisition

The data set used in the experiment was provided by Mumtaz [40]. A total of 34 MDD (17 men, age 40.3/12.9) and 30 NC (21 men, age 38.3/15.6) participated in the experiment. The MDD were from Hospital Universiti Sains Malaysia (HUSM) and met the internationally recognized diagnostic criteria for MDD, the Diagnostic and Statistical Manual (DSM-IV) [40]. Participants with other mental illnesses, smoking, alcohol abuse, etc. that could affect the collection of EEG signals were excluded from MDD, and participants with any mental or physical illnesses were excluded from NC. Prior to the experiment, all subjects were informed of the contents of the experiment and signed informed consent. The experiment was approved by the HUSM ethics committee.

Five minutes of resting EEG were recorded while the eyes were open. Electroencephalogram (EEG) was collected using a 19-

channel EEG cap. The electrodes were placed in an international standard 10–20 system including Fp1, F3, C3, P3, O1, F7, T3, T5, Fz, Fp2, F4, C4, P4, O2, F8, T4, T6, Cz and Pz. The specific locations of the electrodes are shown in Fig. 2. The reference electrode is linked ear (LE) with a sampling frequency of 256HZ. The actual available data downloaded from the website consisted of 28 NC and 30 MDD, of which subjects 14 and 25 in NC and subjects 7, 8, 12 and 34 in MDD were not available.

3.2. Data preprocessing

EEG is susceptible to interference from the environment, devices, and physiological signals. Therefore, prior to the study, EEG needs to be pre-processed to improve the signal-to-noise ratio [16]. Data preprocessing was performed on MATLAB R2019b and the EEGLAB toolbox.

(1) Data filtering: 50HZ notch filtering and 0.5–50HZ band-pass filtering were used to remove low-frequency drift, high-frequency noise and power frequency interference;
(2) Artifact removal: ICA was used to remove artifact signals such as electrooculogram and electromyogram;
(3) Re-reference: re-reference EEG to the whole brain average to reduce the distortion of connection mode;
(4) Data segmentation: Considering the stability of the signal, 100 s EEG after 60 s were extracted for research. The data was segmented in 10s to increase the sample size. Finally, each subject was able to obtain ten pieces of data, the size of each data file was 19×2560 (256×10s), and the total data size was $58 \times 10 = 580$.
(5) Frequency band extraction: zero-phase digital filter was used to extract five sub-bands, delta (0.5-4HZ), theta (4-8HZ), alpha (8-14HZ), beta (14-30HZ) and gamma (30-50HZ). In addition, the performance of total frequency band (0.5–50HZ) in brain network analysis of MDD was also analyzed.

4. Results

4.1. Threshold and density based on at and AD

First, the weighted networks of MDD and NC are computed, and then the binarization thresholds of the weighted networks are calculated using AT and AD. The number of particles and the number of iterations for AT and AD are set to 50 and the results are shown in Table 1. Based on the resulting threshold, the weighted matrix can be transformed into a binary matrix and the functional connectivity difference between MDD and NC can be maximized.

4.2. Comparison of different brain network construction methods

In this paper, seven connectivity methods (Coh, ICoh, MI, PCC, PLI, PLV, WPLI) and four binarization methods (AT, AD, MST, MCC) are used to construct brain networks, so there are a total of 28 method combinations. We then use graph theory to extract five network metrics from brain networks: clustering coefficient, path length, global efficiency, local efficiency, and degree. The binary network obtained by MST is an acyclic connected graph, so the clustering coefficients and local efficiencies of MDD and NC are zero. The binary networks obtained by AD and MST have the same number of connected edges, so the degrees of MDD and NC are equal. According to the computation principle of path length, it can be found that the isolated points influence the path length in the network. Therefore, global efficiency is less disturbed by different combinations of methods. In this paper, we extract the global efficiency from brain networks based on different combinations of methods and analyze the global efficiency of MDD and NC using an independent sample *t*-test and Wilcoxon rank sum test.

The results are shown in Fig. 3, where "*" indicates the statistical difference between MDD and NC. As can be seen in Fig. 3, in the delta band, the results of some combinations show a decrease in the global efficiency of MDD, such as Coh + MCC, while the results of some combinations show an increase in the global efficiency of MDD, such as PLV + AT. In the theta band, the results for partial

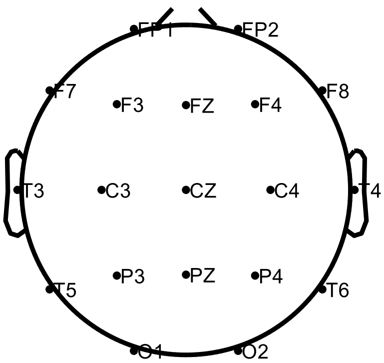

Fig. 2. Specific locations of the electrodes.

Table 1
Results of adaptive threshold and adaptive density.

Con	Bin	delta	theta	alpha	beta	gamma	total
Coh	AT	0.4618	0.8029	0.4818	0.2939	0.3165	0.4929
	AD	0.4624	0.4869	0.4922	0.4868	0.4129	0.3688
ICoh	AT	0.1388	0.3751	0.1006	0.1419	0.1132	0.1372
	AD	0.4980	0.5299	0.4205	0.5146	0.5267	0.5215
MI	AT	0.0772	0.1056	0.0637	0.0225	0.0439	0.0564
	AD	0.3718	0.4757	0.4962	0.4387	0.4322	0.4221
PCC	AT	0.4418	0.5252	0.4327	0.2548	0.2149	0.4401
	AD	0.4696	0.4757	0.5287	0.3809	0.3939	0.4634
PLI	AT	0.2657	0.3031	0.2891	0.2314	0.1704	0.2451
	AD	0.4533	0.3919	0.5025	0.4967	0.5404	0.5208
PLV	AT	0.3611	0.4576	0.3905	0.2478	0.2364	0.3405
	AD	0.5561	0.4397	0.5426	0.4376	0.4553	0.4913
WPLI	AT	0.2677	0.6108	0.3485	0.2618	0.4456	0.2456
	AD	0.4399	0.5280	0.4592	0.5123	0.5131	0.5255

combinations show a decrease in the global efficiency of MDD, as in PLV + AT, while the results for partial combinations show an increase in the global efficiency of MDD, as in PCC + AD. The results for different combinations also show different variations in the alpha, beta, gamma, and full frequency bands. The combination of different methods can affect the construction of the brain network, which then affects the subsequent analysis results. Therefore, it is necessary to construct a reliable method for analyzing MDD brain networks. In addition, the same combination may also exhibit different variation rules in different frequency bands. In PLV + AT, the global efficiency increases significantly in the delta and beta bands and decreases significantly in theta, alpha, gamma, and full bands. Therefore, it is necessary to analyze the changes in the MDD brain network in different frequency bands.

In order to compare the performance of different combinations in the MDD brain network analysis, the number of statistical differences in Fig. 3 are counted, and the results are presented in Table 2. As can be seen from Table 2, PLV + AT corresponds to the largest number of times (number: 6), indicating that there are statistical differences in the global efficiency between MDD and NC in the six frequency bands. When PLV is used to construct the functional connectivity matrix, the number of statistical differences in the global efficiency of MDD and NC is 17, which is higher than other connectivity methods, indicating that PLV may be able to characterize the brain network characteristics of MDD effectively. When AT is used to binarize the functional connectivity matrix, the number of statistical differences in the global efficiency between MDD and NC is 30, which is higher than other binarization methods, indicating that AT may be able to maximize the brain network differences between MDD and NC. In addition, Fscore values for global efficiency are calculated to further evaluate the performance of different combinations, as shown in Table 3. Table 3 shows that the Fscore value of PLV + AT is 0.34, higher than that of other combinations. Comparing the results of different connectivity methods, the Fscore value of PLV is 0.14, which is higher than that of other connectivity methods. Comparing the results of different binarization methods, the Fscore value of AT is 0.26, higher than that of other binarization methods. The results show that PLV + AT is a reliable method for constructing MDD brain networks.

To explore the differences between the MDD and NC brain networks in different frequency bands, the number of statistical differences in the results is counted according to the frequency band, and the results are presented in Table 4. The number of statistical differences in the total frequency band is 22, which is higher than other frequency bands. The number of statistical differences in theta and beta bands is 19 and 18, respectively, ranking second. The most minor statistical differences are seen in the Delta, beta, and gamma bands. The results show that MDD and NC brain networks differ significantly in theta, alpha, and total bands, so theta, alpha, and total bands are favorable for MDD brain network analysis. Therefore, PLV + AT is subsequently used to construct the brain network in this paper, and the changes in the MDD brain network in theta, alpha, and total frequency bands are analyzed.

4.3. Differences in network metrics between NC and MDD

PLV + AT is used to construct MDD brain networks from which cluster coefficients, path lengths, global efficiencies, local efficiencies, and degrees are extracted. The network parameters are statistically tested, and the results are shown in Fig. 4. Fig. 4 shows a statistical difference between the network metrics for MDD and NC in theta, alpha, and full frequency bands, suggesting that the network metrics obtained based on PLV + AT can be used as potential biomarkers for MDD diagnosis. The clustering coefficient and local efficiency of the MDD brain network are lower than that of the NC network, indicating that the local information processing capacity of the MDD brain network is reduced. The path length of the MDD brain network is higher than that of the NC, and the global efficiency is lower than that of the NC, which indicates that the global information transmission capacity of the MDD brain network is reduced. The degree of the MDD brain network is lower than that of the NC network, which indicates that the connections between different regions of the MDD brain network are reduced. The reduced global information transmission and local information processing capacity of the MDD brain network, as well as the reduced connectivity between brain regions, suggest that the MDD brain network is significantly dysfunctional in theta, alpha, and full frequency bands.

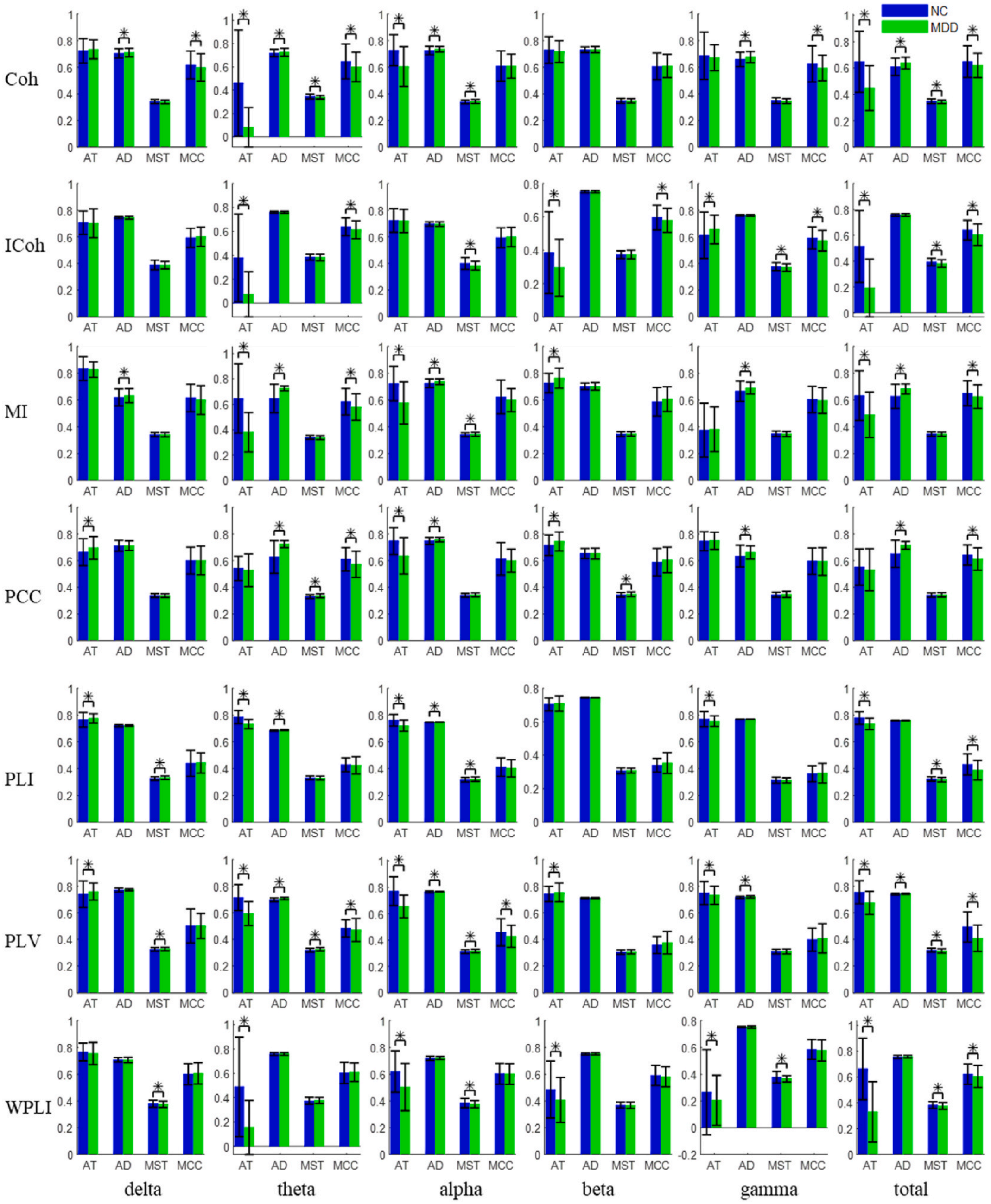

Fig. 3. Statistical test results of global efficiency.

Table 2
Statistical results of different combinations.

Method	AT	AD	MST	MCC	Sum
Coh	3	5	3	4	15
ICoh	4	0	3	4	11
MI	4	5	1	2	12
PCC	3	4	2	2	11
PLI	5	2	3	1	11
PLV	**6**	4	4	3	**17**
WPLI	5	0	4	1	10
Sum	**30**	20	20	17	\

Table 3
Fscore values of different combinations.

Method	AT	AD	MST	MCC	Mean
ICoh	0.25	0.00	0.04	0.04	0.08
Coh	0.26	0.05	0.03	0.02	0.09
MI	0.28	0.17	0.01	0.03	0.12
PCC	0.10	0.19	0.02	0.03	0.08
PLI	0.30	0.06	0.03	0.03	0.11
PLV	**0.34**	0.09	0.05	0.07	**0.14**
WPLI	0.31	0.00	0.03	0.01	0.09
Mean	**0.26**	0.08	0.03	0.03	\

Table 4
Statistical results based on frequency bands.

Bands	delta	theta	alpha	beta	gamma	total
Number	9	**19**	**18**	7	12	**22**

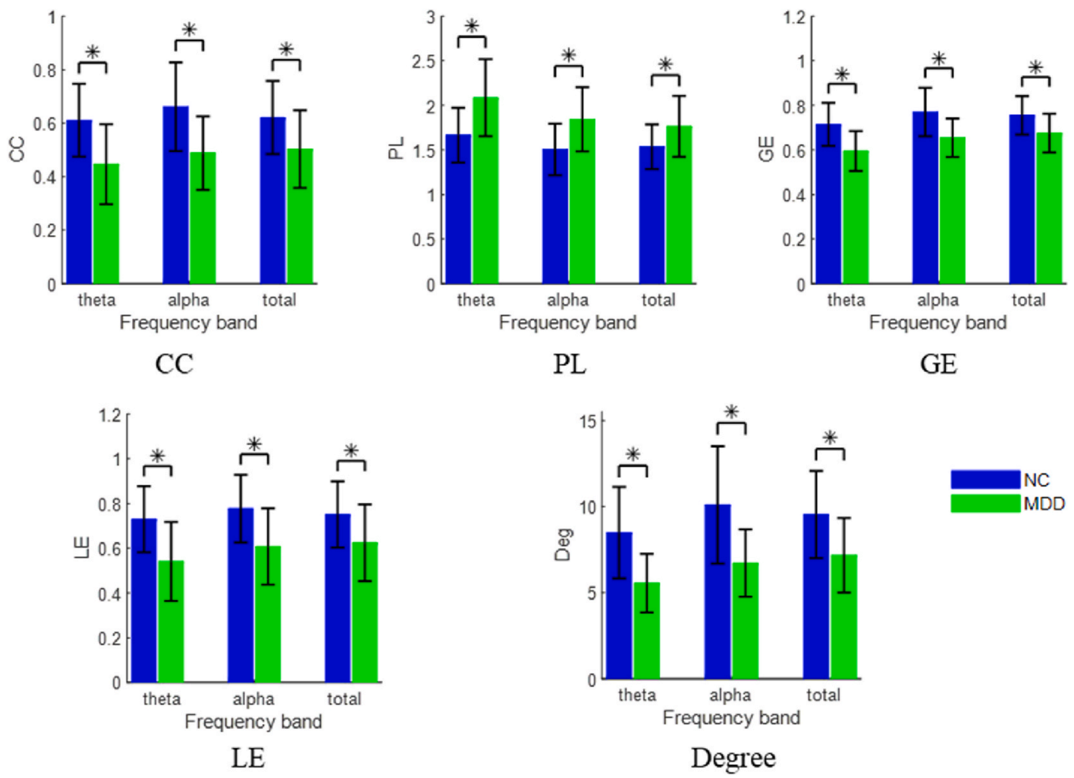

Fig. 4. Statistical test results of network metrics based on PLV + AT.

4.4. Differences in brain topology between NC and MDD

First, PLV is used to compute the functional connectivity matrix, and AT is used to binarize the weighted matrix. Then, the mean matrix of MDD and NC is obtained by averaging the binary matrix of MDD and NC, respectively. When the elements of the mean matrix are greater than 0.5, there is a connection between the electrodes. Otherwise, there is no connection. The brain topology of MDD and NC can be obtained based on the mean matrix. For ease of observation, the brain topology difference maps for MDD and NC are presented, and the results are shown in Fig. 5. Fig. 5 does not show the connection edges that exist in both MDD and NC, but only the different connection edges. From Fig. 5, it can be seen that the number of connected edges in the MDD brain network is significantly lower than that in the NC in the theta, alpha, and total frequency bands, indicating that there may be an obstacle in the information exchange between the MDD brain regions. At the same time, the reduced connectivity of the MDD brain network is evenly distributed between the left and right hemispheres, and no significant hemispheric differences are found.

In order to explore the differences between brain regions, the brain is divided into five brain regions: frontal lobe (Fp1, Fp2, F7, F3, Fz, F4, F8), central lobe (C3, Cz, C4), temporal lobe (T3, T5, T4, T6), parietal lobe (P3, Pz, P4), and occipital lobe (O1, O2). In the delta band, the decrease in the number of connected edges subtracts the increase in the number of connected edges of the MDD brain network. The results are shown in Table 5, where "Sum" only includes changes between brain regions. As can be seen from the changes in the five brain regions, the number of connected edges in the MDD brain network in the frontal lobe decreased by 6, which is significantly higher than the decrease in the other four brain regions. From the changes between brain regions, it can be found that the number of connecting edges between the temporal lobe, as well as the frontal lobe of the MDD brain, and other brain regions decreased by 11 and 10, respectively, which is significantly higher than the other three brain regions. The results suggest that in theta bands, MDD brain dysfunction may be more pronounced in the frontal and temporal lobes.

In alpha and total bands, the number of increased connections subtracts the number of decreased connections in the MDD brain network, and the results are shown in Tables 6 and 7, where "Sum" only includes changes between brain regions. Tables 6 and 7 show that the changes in the MDD brain network in the alpha and total frequency bands are similar to those in the theta band. Regarding changes in connectivity within the six brain regions, the number of connected edges in the MDD brain network decreased the most in the frontal lobe. In terms of changes in connectivity between brain regions, the number of connections between the frontal, as well as temporal lobes, and other brain regions in the MDD brain changed the most. The results showed that MDD had significant brain dysfunction in theta, alpha, and total frequency bands, particularly in the frontal and temporal lobes.

4.5. Brain topographic map analysis

Path length and global efficiency can represent the global properties of the network, while clustering coefficient, local efficiency, and degree can represent the local properties of the network. To analyze the changes in the MDD brain network further, based on the PLV + AT, the global efficiency and node clustering coefficients are extracted from the network. Fig. 6 shows a brain topography map of global efficiency and clustering coefficient. It can be seen from Fig. 6 (a) that the global efficiency of the MDD brain network decreases significantly in the whole brain in theta, alpha, and total frequency bands, indicating that the global information transmission

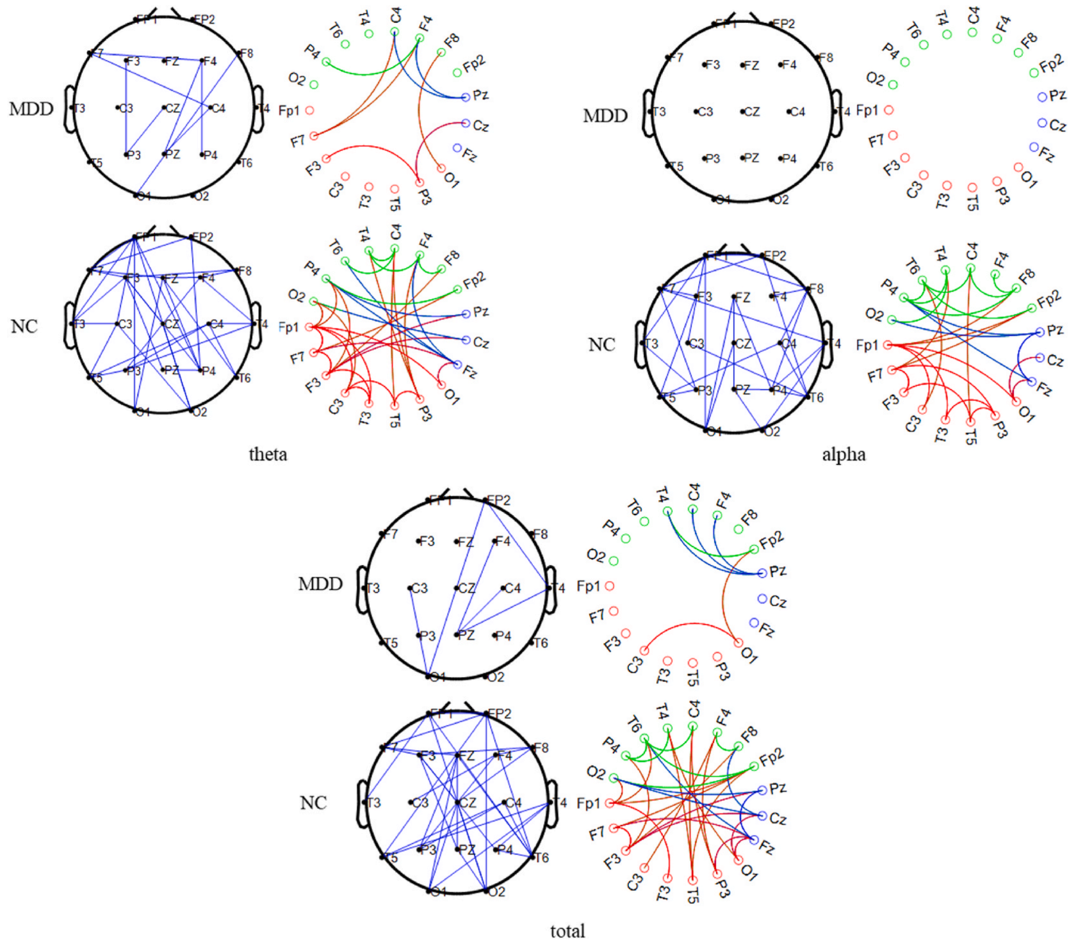

Fig. 5. Brain topology of MDD and NC.

Table 5
Connection edge changes of theta.

Brain	Frontal	Central	Temporal	Parietal	Occipital
Frontal	**6**	1	4	3	2
Central	1	0	5	−1	2
Temporal	4	5	0	2	0
Parietal	3	−1	2	1	0
Occipital	2	2	0	0	0
Sum	**10**	7	**11**	4	4

Table 6
Connection edge changes of alpha.

Brain	Frontal	Central	Temporal	Parietal	Occipital
Frontal	**5**	2	4	4	2
Central	2	0	3	0	1
Temporal	4	3	0	4	1
Parietal	4	0	4	1	1
Occipital	2	1	1	1	0
Sum	**12**	6	**12**	9	5

Table 7
Connection edge changes of total band.

Brain	Frontal	Central	Temporal	Parietal	Occipital
Frontal	**6**	3	4	4	2
Central	3	0	2	0	1
Temporal	4	2	1	1	1
Parietal	4	0	1	0	1
Occipital	2	1	1	1	0
Sum	**13**	6	**8**	6	5

capacity of the MDD brain network decreases. There are two distinct dark blue regions in the MDD brain topography map, located in the left and right temporal lobes, indicating that the temporal lobes of the MDD brain have almost lost the ability to communicate information with other brain regions. It can be seen from Fig. 6 (b) that in theta, alpha, and total frequency bands, clustering coefficient of the MDD brain network decreased significantly in the whole brain, indicating that the local information processing ability of the entire MDD brain network had a downward trend. There are distinct dark blue regions in the left and right temporal lobes of the MDD brain topography map, suggesting that the temporal lobes of the MDD brain have almost lost their ability to process local information. The results show that the MDD brain network has lower global information transfer and local information processing capacity than the NC network, especially in the temporal lobe.

4.6. Effects of different genders on brain networks

In order to make full use of the characteristic information of the subjects, we grouped the data according to gender. The PLV + AT method was used to construct the brain function network, and the brain network metrics of males and females were statistically analyzed. The results are shown in Fig. 7. The M represents male, and F represents female. It can be found from the figure that in different genders, the clustering coefficient, global efficiency, local efficiency, and degree of MDD brain network in different frequency bands are lower than that of NC, and the path length is greater than that of NC. Therefore, the changing trend of MDD brain network metrics was the same in different genders. In addition, the brain network metrics of males and females in the group were statistically analyzed. In the theta band of the NC group, the clustering coefficient, global efficiency, local efficiency, and degree of the female brain network were higher than that of the male brain network, and the path length was lower than that of the male brain network. In the alpha band of the MDD group, the clustering coefficient, global efficiency, local efficiency, and degree of the female brain network were smaller than that of the male brain network, and the path length was larger than that of the male brain network. In the alpha band of the NC group and the total band of the MDD group, there were no significant differences in all brain network metrics between males and females. The results showed significant differences in the brain networks of males and females in some frequency bands, especially in the theta (NC) and alpha (MDD) bands.

5. Discussion and limitation

In this paper, we explore the performance of different connectivity and binarization methods in constructing brain networks, and construct a reliable method for MDD brain network analysis. The results show that PLV + AT is a reliable method for constructing MDD

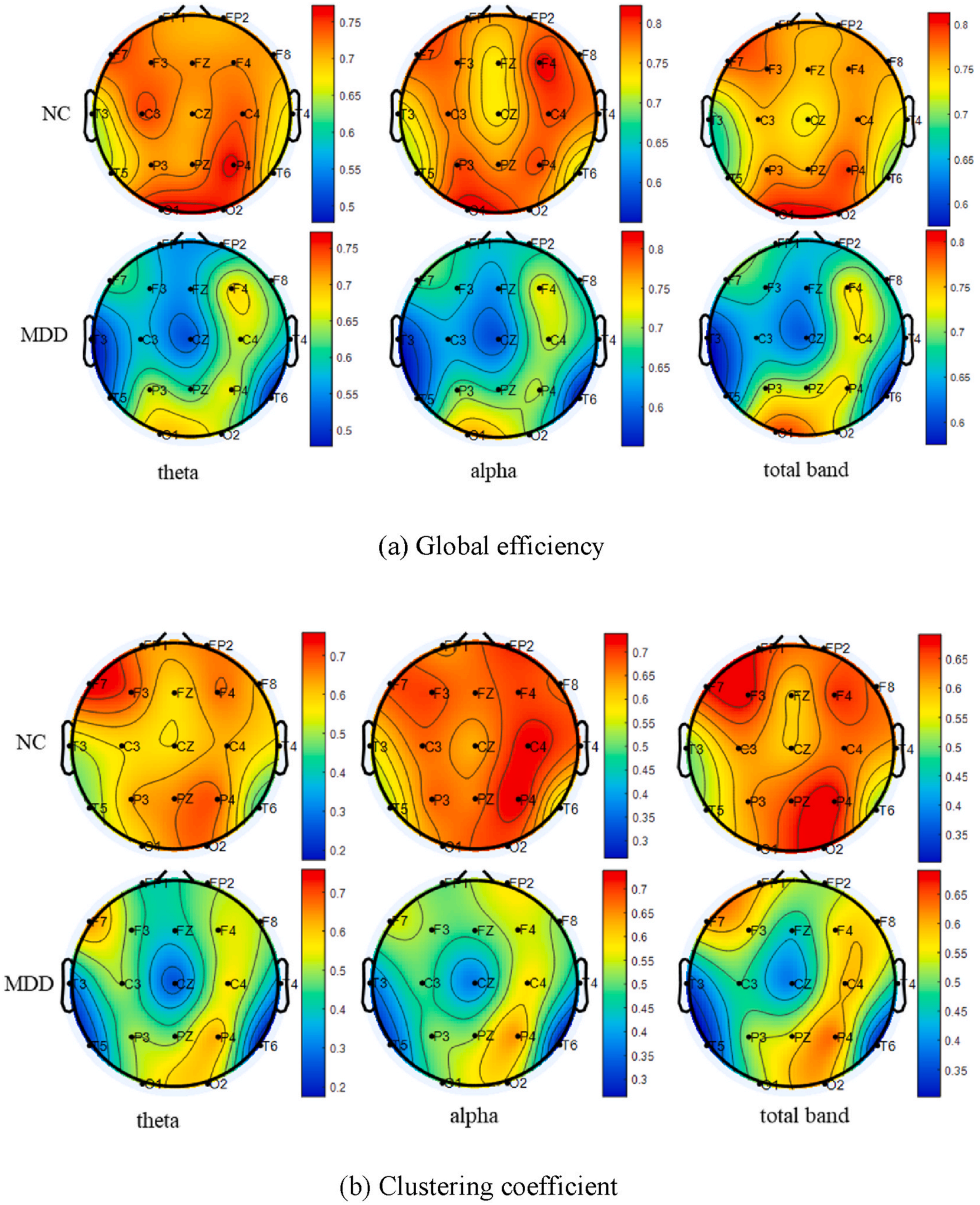

Fig. 6. Brain topographic map of global efficiency and clustering coefficient.

brain networks, and the differences between MDD and NC brain networks in theta, alpha and total frequency bands are clear. Based on PLV + AT, graph theory is used to analyze the changes in the MDD brain network. The results show that MDD brain network is dysfunctional, particularly in the frontal and temporal lobes.

The MDD brain network is constructed using 28 combinations of seven connectivity methods (Coh, ICoh, MI, PCC, PLI, PLV, WPLI) and four binarization methods (AT, AD, MST, MCC). Global efficiency is extracted from the brain network to compare the performance of different combinations in the MDD brain network analysis. The global efficiency is then statistically tested, and the number of statistical differences in the results is counted. PLV shows the highest number of statistical differences among the seven connectivity methods. AT shows the highest number of statistical differences among the four binarization methods. PLV + AT shows the highest number of statistical differences among the 28 combinations. The Fscore values for the different combinations are also calculated. The Fscore of PLV is higher than that of other connectivity methods, the Fscore of AT is higher than that of other binarization methods, and the Fscore of PLV + AT is higher than that of other combinations. The results show that PLV + AT is a reliable MDD brain network

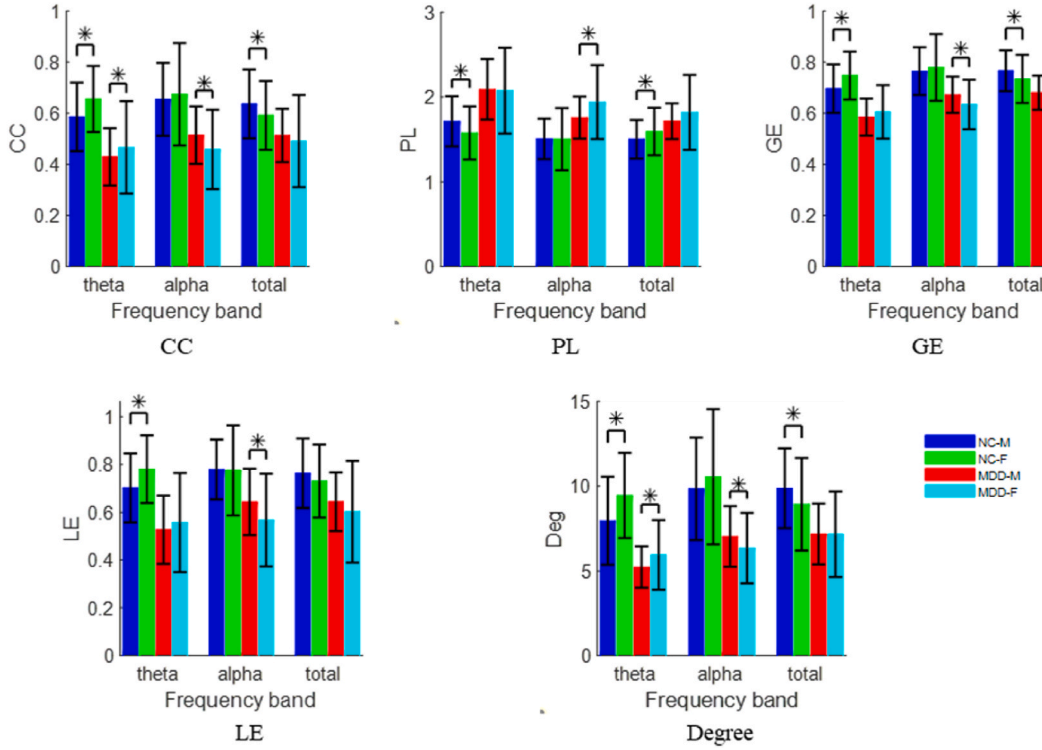

Fig. 7. Results of statistical tests grouped with gender.

analysis method. Meanwhile, AT performs better than other binarization methods in MDD brain network analysis, indicating that the adaptive threshold method based on QPSO can realize the binarization of weighted networks and maximize the difference between MDD and NC brain networks, which is conducive to MDD brain network analysis, and verifies the superiority of AT. Moreover, the differences between MDD and NC brain networks in different frequency bands are analyzed, and it is shown that MDD and NC brain networks differ significantly in theta, alpha, and total frequency bands.

Based on PLV + AT, a brain network is constructed in theta, alpha, and total frequency bands, from which clustering coefficient, path length, global efficiency, local efficiency, and degree are extracted. The statistical test results show that all network metrics of the MDD brain network are statistically different from those of the NC in theta, alpha, and total frequency bands, suggesting that PLV + AT based network metrics may be the potential biological indicators for MDD identification. The clustering coefficient, global efficiency, local efficiency, and degree of the MDD brain network are lower than NC, and the path length is higher than NC, which indicates that the global information transmission ability and local information processing ability of the MDD brain network are significantly decreased in theta, alpha, and total frequency bands. Zhang et al. [18] found that in the theta band, the clustering coefficient of MDD decreases, and the path length increases. Sun et al. [24] pointed out that theta and alpha bands performed better in MDD brain network analysis and found that the clustering coefficient of MDD decreased significantly in theta band. Shim et al. [41] pointed out that the clustering coefficient of MDD in theta and alpha bands decreased while the path length in the alpha band increased. Most studies indicate that the brain network of MDD has significant changes in theta and alpha bands [18,24], which is consistent with the results of this study. However, few studies have discussed MDD brain network changes in the total frequency band. The results of this paper show that the brain network of MDD also shows significant changes in the total frequency band.

In theta, alpha, and total frequency bands, the brain topology of MDD and NC is analyzed, and it is found that the functional connectivity of MDD is significantly lower than that of NC, indicating the dysfunction of the MDD brain network. The brain was further divided into frontal, central, temporal, parietal, and occipital lobes to explore the differences between different brain regions. The results show that the connectivity edges in the frontal lobes of MDD are significantly reduced compared to NC brain networks, and the connectivity edges between the frontal, as well as temporal lobes, and other brain regions of MDD are significantly reduced. After that, the brain topography map based on global efficiency and clustering coefficient are analyzed. The results show a downward trend in global information transmission and local information processing in the MDD brain across brain regions. In the temporal lobe, the MDD brain has almost no information transmission and processing functions. The results showed that the MDD brain was dysfunctional, particularly in the frontal and temporal lobes. Existing studies have also shown that the main regions of brain dysfunction in MDD may be the frontal and temporal lobes [13]. Sun et al. [24] pointed out that the frontal lobe is related to MDD. Zhang et al. [42] used four EEG signals in the temporal lobe to realize the diagnosis of MDD. The results of this study provide further evidence that the frontal and temporal lobes are involved in MDD.

The effects of gender on brain networks were further studied in this paper. The results showed that the changing trend of the MDD brain network was the same when gender was different, indicating that gender did not affect the changing trend of the MDD brain network. Therefore, there is no gender discrimination in the study of MDD brain network changes. The comparison of male and female brain networks within the group showed significant differences in brain networks in some frequency bands, such as theta band in the NC group and the alpha band in the MDD group. Therefore, if gender can be distinguished for MDD diagnosis, the accuracy of MDD diagnosis may be improved.

This paper proposed a reliable method of MDD brain network construction, and the trend of MDD brain network change was analyzed, which provided a basis for MDD brain analysis and MDD diagnosis. The results showed that the MDD brain network construction method based on PLV + AT had high reliability and could fully characterize the differences between NC and MDD brain networks, which was conducive to MDD brain network analysis and MDD diagnosis. Statistical analysis showed that MDD brain networks were dysfunctional, especially in the frontal and temporal lobes of the theta, alpha, and total bands. Therefore, in the diagnosis of MDD, we can pay more attention to critical frequency bands and brain regions to reduce the number of EEG collection electrodes and increase the feasibility of MDD diagnosis methods. In addition, the brain networks of males and females differed significantly in some frequency bands. Therefore, in MDD diagnosis, gender differentiation can be considered when establishing the MDD diagnosis model to improve the accuracy of MDD diagnosis.

There are some limitations in this study. First, the small number of channels in the dataset makes it challenging to explore hemispheric differences in MDD brains further. Future work could analyze MDD brain network changes on 64 or 128 channel datasets to further analyze left-right hemispheric differences. Second, this paper focuses on analyzing the changes in the MDD brain network under resting state EEG. In the future, we can explore the differences in MDD brain networks between task-state EEG and resting-state EEG. Third, this paper only explored the changes in the brain network and did not explore the MDD diagnosis methods. Based on the research work in this paper, a machine learning-based MDD diagnosis method can be proposed in the future. Based on the proposed method in this paper, future research focuses on extracting comprehensive features from brain networks and building effective classifiers for classification.

6. Conclusion

In this paper, we compare the performance of different connectivity and binarization methods in brain network construction and construct a reliable MDD brain network analysis method. The results show that PLV + AT is a reliable MDD brain network analysis method. Meanwhile, the AT algorithm based on QPSO can achieve adaptive threshold setting and maximize the difference between MDD and NC brain networks, which is better than existing binarization methods. Based on PLV + AT, the network metrics, brain topology maps, and brain topography maps of MDD and NC are compared and analyzed. The results suggest that PLV + AT based network metrics may be potential biological metrics for MDD identification. At the same time, the clustering coefficient, the global efficiency, the local efficiency, and the degree of MDD decrease, and the path length increases, indicating that the global information transmission and the local information processing capacity of MDD brain networks decrease. The number of connected edges in the MDD brain network decreases, especially in the frontal and temporal lobes. In summary, this study suggests that there is dysfunction in the MDD brain, especially in the frontal and temporal lobes.

Data availability

All Data files are available from the (http://figshare.com/) database https://figshare.com/articles/EEG_Data_New/4244171.

CRediT authorship contribution statement

Wan Chen: Writing – original draft, Validation, Methodology, Investigation, Data curation, Conceptualization. **Yanping Cai:** Writing – review & editing, Methodology, Conceptualization. **Aihua Li:** Writing – review & editing, Validation, Methodology. **Ke Jiang:** Writing – review & editing, Validation. **Yanzhao Su:** Writing – review & editing, Validation.

Declaration of competing interest

The authors declare that they have no known competing financial interests or personal relationships that could have appeared to influence the work reported in this paper.

References

[1] L. Yang, Y. Wang, X. Zhu, et al., A gated temporal-separable attention network for EEG-based depression recognition, Comput. Biol. Med. 157 (2023) 106782.
[2] J. Zhu, Z. Wang, T. Gong, et al., An improved classification model for depression detection using EEG and eye tracking data, IEEE Trans. NanoBioscience 19 (3) (2020) 527–537.
[3] R. Movahed, G. Jahromi, S. Shahyad, et al., A major depressive disorder classification framework based on EEG signals using statistical, spectral, wavelet, functional connectivity, and nonlinear analysis, J. Neurosci. Methods 358 (2021) 109209.
[4] M. Xia, Y. Zhang, Y. Wu, et al., An end-to-end deep learning model for EEG-based major depressive disorder classification, IEEE Access 11 (2023) 41337–41347.
[5] Z. Wang, J. Feng, R. Jiang, et al., Automated rest EEG-based diagnosis of depression and schizophrenia using a deep convolutional neural network, IEEE Access 10 (2022) 104472–104485.
[6] A. Seal, R. Bajpai, A. Yazidi, et al., A deep convolution neural network framework for detecting depression using EEG, IEEE Trans. Instrum. Meas. 70 (2021) 2505413.

[7] B. Wang, Y. Kang, D. Huo, et al., Depression signal correlation identification from different EEG channels based on CNN feature extraction, Psychiatr. Res. Neuroimaging 328 (2023) 111582.
[8] H. Chiang, M. Chen, L. Liao, Cognitive depression detection cyber-medical system based on EEG analysis and deep learning approaches, IEEE Journal of Biomedical and Health Informatics 27 (2) (2023) 608–616.
[9] A. Khadidos, K. Alyoub, S. Mahato, et al., Computer aided detection of major depressive disorder (MDD) using electroencephalogram signals, IEEE Access 11 (2023) 41133–41141.
[10] J. Yang, Z. Zhang, Z. Fu, et al., Cross-subject classification of depression by using multiparadigm EEG feature fusion, Comput. Methods Progr. Biomed. 233 (2023) 107360.
[11] C. Greco, O. Matarazzo, G. Cordasco, et al., Discriminative power of EEG-based biomarkers in major depressive disorder: a systematic review, IEEE Access 9 (2021) 112850.
[12] Y. Li, D. Gao, L. Wei, et al., Abnormal functional connectivity of EEG gamma band in patients with depression during emotional face processing, Clin. Neurophysiol. 126 (11) (2015) 2078–2089.
[13] X. Li, Z. Jing, B. Hu, et al., A resting-state brain functional network study in MDD based on minimum spanning tree analysis and the hierarchical clustering, Complexity 2017 (2017) 9514369.
[14] W. Liu, C. Zhang, X. Wang, et al., Functional connectivity of major depression disorder using ongoing EEG during music perception, Clin. Neurophysiol. 131 (2020) 2413–2422.
[15] R. Kalpana, I. Gnanambal, The Analysis of nonlinear invariants of multi-channel EEG signal using graph-theory connectivity approach in patient with depression, Asian J. Inf. Technol. 15 (20) (2016) 4106–4112.
[16] Y. Xie, B. Yang, M. Zheng, et al., Anxiety and depression diagnosis method based on brain networks and convolutional neural networks. 2020 42nd Annual International Conference of the IEEE Engineering in Medicine & Biology Society, EMBC), 2020 19964516.
[17] X. Shao, S. Sun, J. Li, et al., Analysis of functional brain network in MDD based on improved empirical mode decomposition with resting state EEG data, IEEE Trans. Neural Syst. Rehabil. Eng. 29 (2021) 1546–1556.
[18] B. Zhang, G. Yan, Z. Yang, et al., Brain functional networks based on resting-state EEG data for major depressive disorder analysis and classification, IEEE Trans. Neural Syst. Rehabil. Eng. 29 (2021) 215–229.
[19] M. Jalili, Functional brain networks: does the choice of dependency estimator and binarization method matter? Sci. Rep. 6 (2016) 29780.
[20] S. Sun, L. Liu, X. Shao, et al., Abnormal brain topological structure of mild depression during visual search processing based on EEG signals, IEEE Trans. Neural Syst. Rehabil. Eng. 30 (2022) 1705–1715.
[21] B. Zhang, H. Cai, Y. Song, et al., Computer-aided recognition based on decision-level multimodal fusion for depression, IEEE Journal of Biomedical and Health Informatics 26 (7) (2022) 3466–3477.
[22] M. Zhang, H. Zhou, L. Liu, et al., Randomized EEG functional brain networks in major depressive disorders with greater resilience and lower rich-club coefficient, Clin. Neurophysiol. 129 (4) (2018) 743–758.
[23] W. Mumtaz, S. Ali, M. Yasin, et al., A machine learning framework involving EEG-based functional connectivity to diagnose major depressive disorder, Med. Biol. Eng. Comput. 56 (2) (2018) 233–246.
[24] S. Sun, X. Li, J. Zhu, et al., Graph theory analysis of functional connectivity in major depression disorder with high-density resting state eeg data, IEEE Trans. Neural Syst. Rehabil. Eng. 27 (3) (2019) 429–439.
[25] W. Liu, X. Wang, J. Xu, et al., Identifying oscillatory hyperconnectivity and hypoconnectivity networks in major depression using coupled tensor decomposition, IEEE Trans. Neural Syst. Rehabil. Eng. 29 (2021) 1895–1904.
[26] X. Li, Y. Wu, M. Wei, et al., A novel index of functional connectivity: phase lag based on Wilcoxon signed rank test, Cognitive Neurodynamics 15 (4) (2020) 621–636.
[27] B. He, L. Astolfi, P. Valdes-Sosa, et al., Electrophysiological brain connectivity: theory and implementation, IEEE (Inst. Electr. Electron. Eng.) Trans. Biomed. Eng. 66 (7) (2019) 2115–2137.
[28] X. Liu, S. Liu, M. Li, et al., Altered gamma oscillations and beta-gamma coupling in drug-naïve first-episode major depressive disorder: association with sleep and cognitive disturbance, J. Affect. Disord. 316 (2022) 99–108.
[29] L. Ismail, W. Karwowski, A graph theory-based modeling of functional brain connectivity based on EEG: a systematic review in the context of neuroergonomics, IEEE Access 8 (2020) 155103–155135.
[30] X. Li, R. La, Y. Wang, et al., A deep learning approach for mild depression recognition based on functional connectivity using electroencephalography, Front. Neurosci. 14 (2020) 192.
[31] F. Hasanzadeh, M. Mohebbi, R. Rostami, Graph theory analysis of directed functional brain networks in major depressive disorder based on EEG signal, J. Neural. Eng. 17 (2) (2020) 026010.
[32] G. Fraga, M.J.W. Van, G. Zaric, et al., Graph analysis of EEG resting state functional networks in dyslexic readers, Clin. Neurophysiol. 127 (9) (2016) 3165–3175.
[33] R. Vijayalakshmi, D. Nandagopal, N. Dasari, et al., Minimum connected component - a novel approach to detection of cognitive load induced changes in functional brain networks, Neurocomputing 170 (2015) 15–31.
[34] L. Yang, X. Wei, F. Liu, et al., Automatic feature learning model combining functional connectivity network and graph regularization for depression detection, Biomed. Signal Process Control 82 (2023) 104520.
[35] J. Shen, X. Zhang, X. Huang, et al., An optimal channel selection for EEG-based depression detection via kernel-target alignment, IEEE Journal of Biomedical and Health Informatics 25 (7) (2021) 2545–2556.
[36] R. Xue, R. Zhao, The fault feature selection algorithm of combination of ReliefF and QPSO, J. Vib. Shock 39 (11) (2020) 171–176.
[37] Z. Cui, X. Geng, Support vector machine algorithm based on random forest and quantum particle swarm optimization, Comput. Integrated Manuf. Syst. 29 (9) (2023) 2929–2936.
[38] H. Mohammed, M. Diykh, Improving EEG major depression disorder classification using FBSE coupled with domain adaptation method based machine learning algorithms, Biomed. Signal Process Control 85 (2023) 104923.
[39] C. Wu, D. Dillon, H. Hsu, et al., Depression detection using relative EEG power induced by emotionally positive images and a conformal kernel support vector machine, Appl. Sci. 8 (8) (2018) 1244.
[40] W. Mumtaz, L. Xia, M. Yasin, et al., A wavelet-based technique to predict treatment outcome for major depressive disorder, PLoS One 12 (2) (2017) 0171409.
[41] M. Shim, C. Im, Y. Kim, et al., Altered cortical functional network in major depressive disorder: a resting-state electroencephalogram study, Neuroimage: Clinic 18 (2018) 1000–1007.
[42] Y. Zhang, K. Wang, Y. Wei, et al., Minimal EEG channel selection for depression detection with connectivity features during sleep, Comput. Biol. Med. 147 (2022) 105690.